2016 13th International Multi-Conference on Systems, Signals & Devices

Reliability Analysis of Distribution Systems with Hybrid Renewable Energy and Demand Side Management

Maad Al Owaifeer
Electrical Engineering Department
King Fahd University of Petroleum and Minerals
Dhahran, Saudi Arabia
alowaifeer@kfupm.edu.sa

Mohammad AlMuhaini
Electrical Engineering Department
King Fahd University of Petroleum and Minerals
Dhahran, Saudi Arabia
muhaini@kfupm.edu.sa

***Abstract*—Reliability is, and will always be, a crucial mater in designing efficient smart distribution systems. Although renewable based DGs can largely improve the figure of reliability, they may also harm it due to their fluctuating nature. One of the key characteristics of smart distribution systems that could resolve this issue is the demand side management (DSM). DSM refers to any activity done by the utility or the customer to influence load behavior. There are many effective aspects of the DSM that, when addressed efficiently, could benefit both utilities and consumers.**

In this paper, a reliability assessment of a smart distribution local load system will be studied, including the DSM and the integration of wind and solar energies. The impact of the wind and solar energies on the reliability of the local load will be addressed and compared to base-case reliability. Actual wind speed data and solar irradiation are used in modeling wind and solar power outputs to include seasonal variations. Then, the DSM concept will be implemented to assess the increase in load reliability. Two main DSM aspects are studied and simulated which are load shifting and peak clipping aspects. The Monte Carlo Simulation (MCS) will be utilized to evaluate the reliability for residential, commercial, and industrial loads.

***Index Terms*— Reliability, Wind Power, PV Energy, Hybrid Systems, Demand Side Management, Monte Carlo Simulation**

I. Introduction

Conventional DGs and renewable energy (RE) based DGs play an important role in enhancing the reliability of restoration process. This is due to their ability to serve loads connected nearby during faulted hours. However, if the capacity of the DG or the current output of RE resources is relatively low during a failure, far connected loads will not be restored. This issue can be solved through controlling the loads by applying demand side management (DSM) actions. An operator can find and apply an optimum load management scheme that is able to restore more loads and minimize the interruption cost. Furthermore, operators can forecast RE outputs and implement DSM programs based on the forecasted results. Hence, the combination of DSM and RE becomes a crucial mater for increasing system reliability.

Although several papers study the effect of RE and DSM, separately, on the reliability, the literature still lacks researches combining the two aspects together. Very few papers ad-dressed the impacts of combining RE and DSM [1, 2]. Reference [1] examined the effect of selected load management techniques with wind power on the individual load point and system reliability indices. However, when modeling load shifting technique, the load was assumed to be always constant at peak hours which limits the practicality. In [2], simulation studies have been performed on real Italian distribution network, showing the effects of DSM actions on the growth of DGs. However, the wind generator used in the study was assumed to be equivalent to a constant generator excluding the stochastic nature of wind speed.

In this paper, the impact of the wind and solar energies on the reliability of a local load will be addressed and compared to base case reliability. Then, the DSM concept will be implemented to assess the increase in load reliability. The Monte Carlo simulation (MCS) will be utilized to evaluate the reliability for residential, commercial, and industrial loads. As shown in Fig.1, four different stages will be considered in this paper. The first stage of study will be the base case where the load is connected to only the utility. The second stage is when the hybrid renewable DG is integrated to the system. The third stage is when DSM is applied to connected loads where the dashed data line in Fig. 1 simulates the information exchange between utility and consumer. The fourth and final stage is when the DSM is implemented to the system including hybrid renewable DG.

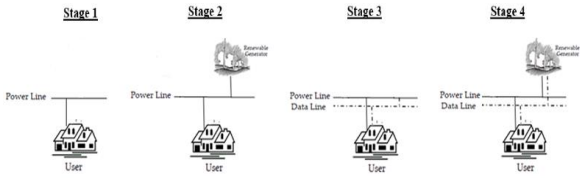

Fig 1. Stages of study considered in this paper (the dashed line (DATA Line) on the right refers to the DSM prectice [3])

978-1-5090-1291-6/16/$31.00 ©2016 IEEE

II. System Modeling

A. Load modeling

The mechanism of building the hourly load model used in this study is clearly illustrated in [4]. This model simulates the hourly load behavior for different sectors based on the hour of the day, the day of the week, and the week of the year. The per unit hourly load model can then be extracted by the following equation:

$$\text{Load}(t) = \text{Ph}\times\text{Pd}\times\text{Pw} \tag{1}$$

where Load(t) is the load at hour t in per unit, Ph, Pd, and Pw are the load factors for hour t in the year, h is hour of the day (1-24), d is day of the week (1-7), and w is week of the year (1-52).

To further simulate the uncertainty of the load, in this paper, each load point is generated randomly based on a normal distribution function with the mean equal to the multiplication of the factors (weekly, daily, and hourly) for that load point. Usually, in long-term load forecasting, the relative errors between the actual and the forecasted values range below 15% ([5],[6]). To simulate that error, 15% of the mean at each load point is set to equal three standard deviations, meaning that the maximum deviation from the mean value is ≈15%. The following equations are used to simulate the load for different sectors such as residential, commercial, and industrial loads.

$$\begin{aligned} m(t) &= \text{Ph}\times\text{Pd}\times\text{Pw} \\ 3\sigma(t) &= 15\% \times m(t) \\ \text{Load}(t) &= \text{normrand}(m(t),\sigma(t)) \end{aligned} \tag{2}$$

where m(t) is the mean used to generate the load at hour t, σ(t) is the standard deviation for hour t, and "normrand" is a normal random generator.

B. Modeling renewable energies power output

1) Wind turbine (WT) power output

Wind turbines are currently available with a variety of power sizes, depending on the application that they will be used for, and the type of load to be connected with. Practically speaking, the power output of a wind turbine depends mainly on the speed of the wind and which can be expressed by the following sub-functions [7]:

$$P_{\text{out}}(v) = \begin{cases} 0, & v \le v_{ci} \cup v \ge v_{co} \\ P_{\text{R}} \dfrac{v^3 - {v_{ci}}^3}{{v_R}^3 - {v_{ci}}^3}, & v_{ci} < v < v_R \\ P_{\text{R}}, & v_R \le v \le v_{co} \end{cases} \tag{3}$$

where v is the wind speed, v_{ci} is the cut-in speed (minimal speed for output power), $v_R$is the rated output speed, v_{co} is the cut-out speed (maximum speed for outputting power), P_R is the rated output power, and P_{out} is the output power of the wind turbine.

When choosing a specific wind turbine to be installed, the wind speed at the location of installation should be carefully studied. These studies are made to optimize the wind power output and to minimize operational cost.

For this study, historical hourly wind speed data for the studied location were analyzed to decide which wind turbine would generate more sustained power. By fitting the wind speed data in a Weibull distribution function (Fig. 2), the appropriate parameters of the selected wind turbine were specified and are listed in Table I. Based on the hourly actual wind speed data, the output power of the chosen wind turbine for one year was calculated using equation 3. Then the hourly averaged power output values were converted to a per-unit system on a base of the maximum power output of the WT to match the load scale (Load_{max}=1p.u.).

2) Photovoltaic (PV) cells power output

The power output from the PVs is influenced by many external factors such as temperature and sunlight intensity. A simplified equation that relates the sun irradiation and the PV power output is as follows [7].

$$P_{out} = P_{STC}\frac{G_{AC}}{G_{STC}} \tag{4}$$

where P_{STC} is the maximum test power for the STC (standard test conditions: solar irradiation 1000W/m2, ambient temperature 25C°).
G_{AC} is the simulated solar irradiation in (W/m^2)
$G_{STC}$is the solar irradiation for the STC = 1000 W/m^2 [7].

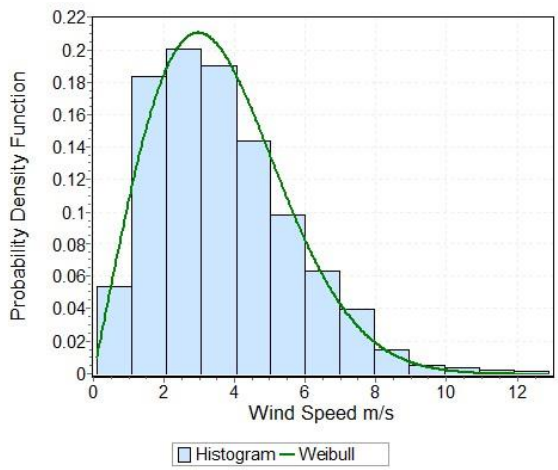

Fig 2. Weibull Distribution for the Studied Wind Speed

TABLE I. Wind Turbine Parameters

v_{ci}	1.2 m/s
v_R	9 m/s
v_{co}	25 m/s
P_R	11 KW

In this study, the maximum test power (P_{STC}) will be equal to 1 p.u. to match the load scale as in the case of wind power output. Similar to the wind speed date, actual hourly solar irradiation data were obtained from the same location of the wind speed data. Then, equation 4 was used to calculate the PV power output.

C. Modeling demand side management (DSM)

Two DSM aspects are simulated in this paper. These are, load shifting LS and peak clipping PC. The DSM modeling used in this paper is explicitly illustrated in [8]. It was achieved by introducing two factors, the shifting factor N and the clipping factor C. The former represents the effectiveness of load shifting and the latter represent the effectiveness of peak clipping. Figs. 3 and 4 demonstrate the methodology.

D. Fail and repair incidents simulation by MCS

After generating the hourly load data for a complete year, fail incidents and repair actions of the system were simulated using Monte Carlo Simulation. Generally, the probability to fail or repair for an electrical system follows an exponential distribution, which is what will be used in the simulation process. It is assumed in this study that the system is having a failure rate of 4 f/yr and a mean time to repair of 4 hours. The sample simulation procedure is implemented as follows:

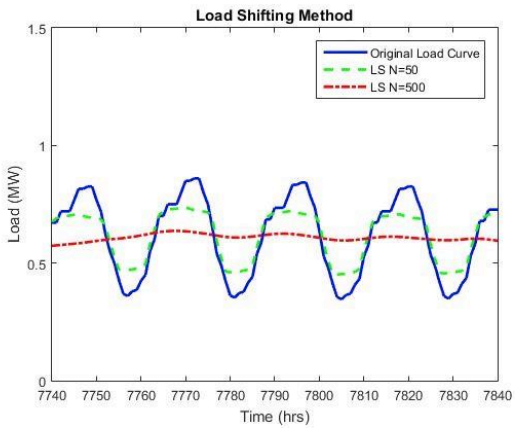

Fig 3. Load shifting method

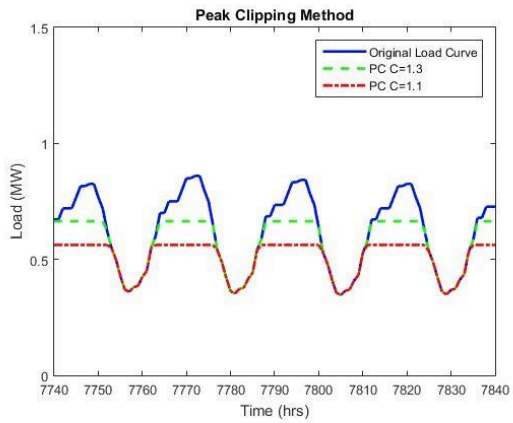

Fig 4. Peak Clipping Method

$$\text{if CDF(t)} > \text{random(0-1)} \longrightarrow \text{incident occur}$$
$$\text{else} \longrightarrow \text{incident did not occur} \qquad (5)$$

where CDF is the Cumulative Distribution Function of the exponential distribution, "random" generates a random number between (0,1), and t is time in hours for a complete year.

The detailed implementation of the MCS is illustrated in a flow chart in Fig.5. This procedure will be used to simulate and ex-tract the fail and repair hours for the case study in the following section.

III. Procedure of Analysis

The study was applied on a part of the RBTS system [9] considering three local load types, residential, commercial, and industrial that are connected through the same feeder. Four main stages are considered in this study: the base case, renewable energy integration, implementing DSM, and finally, applying DSM with the integration of renewable energy. At each stage, the reliability will be evaluated using two indices as a measure. These two indices are the Unavailability in hours and the Energy Not Supplied (ENS) in per unit considering the load energy peak to be the base. The unavailability at each hour is calculated as shown in equation (6).

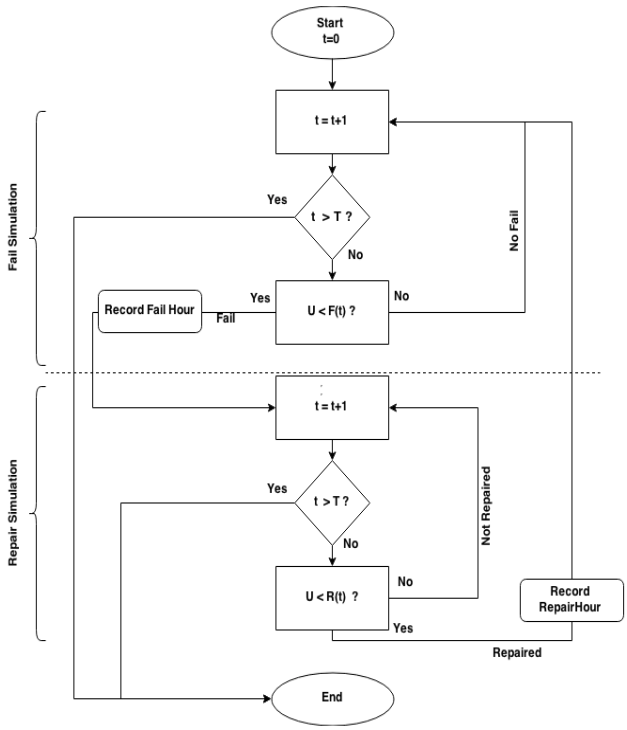

Fig 5. MCS Implementation Procedure

Where t: simulated hour in the year
T: Total number of simulated hours in the year.
U: normal random generator between 0-1.
F(t): failure CDF = $1 - e^{-\lambda t}$;λ: failure rate of the local load.
R(t): repair CDF = $1 - e^{-\mu t}$; μ: repair rate of the local load

$$U(t) = \begin{cases} 0, & P_S(t) \geq R \times P_D(t) \\ 1, & P_S(t) < R \times P_D(t) \end{cases} \quad (6)$$

for all t.

where $U(t)$ is the unavailability at hour t, $P_S(t)$ is the power supply at hour t, $P_D(t)$ is the demand at hour t, and R is the curtailment level in % that specifies when to consider the generation unavailable. For example, if R is 75%, the generation is unavailable if it, at least, cannot meet 75% of the demand.

Then, by summing all $U(t)$, we get the total unavailability in hours.

The ENS at each hour is calculated as follows:

$$ENS(t) = \begin{cases} 0 & , P_S(t) \geq P_D(t) \\ P_D(t) - P_S(t), & P_S(t) < P_D(t) \end{cases} \quad (7)$$

for all t.

where $ENS(t)$ is the energy not supplied at hour t.

Then, by summing all $ENS(t)$, we get the total ENS in p.u.

A flow chart that summarizes the paper procedure is shown in Fig.6 Renewable energy stage will include integrating wind turbine and PV cells simultaneously. Also, DSM stage will include LS and PC methods. A total of 6 cases are studied by interchanging the integrated RE and the applied DSM method as illustrated in table II.

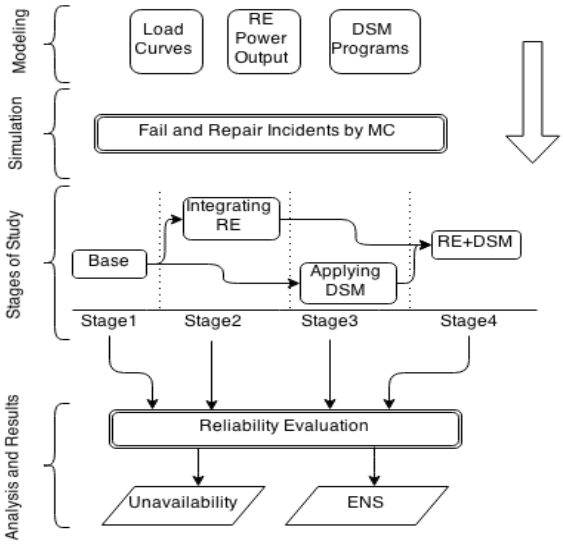

Fig 6. General Architecture Flow Chart of the Paper

TABLE II. TOTAL STUDIED CASES

		RE		DSM	
	Case	WT	PV	LS	PC
Stage1	1				
Stage2	2	✓	✓		
Stage3	3			✓	
	4				✓
Stage4	5	✓	✓	✓	
	6	✓	✓		✓

IV. RESULTS AND DISCUSSION

A. Stage1. Base case; load connected to utility only

The system in this case is considered to be the base, where there is no DG connected and the DSM is not yet included. After running the fail and repair simulation shown in Fig. 6, 6 failures occurred. Table III lists in detail the time of each interruption. Table IV shows the total unavailability and the ENS during the failures for each load type. Obviously, ENS differs for each load type since they consume different amount of energies at different times while the unavailability is similar in all load sectors.

B. Stage 2. Integrating hybrid renewable energies

RE DGs are connected at each studied load point where during system interruption, each load is isolated from the system and operated in islanded mode with its own hybrid system which include wind and solar power.

Table V lists the ENS, and Fig. 7 shows the Unavailability.

The ENS decreased for the residential, commercial, and Indus-trial loads by 83.42%, 69.1%, and 66.6%, respectively, com-pared to the base case. This shows the effectiveness of RE in retrieving lost loads.

C. Stage3. Applying demand side management (DSM)

It is important to note out that the unavailability index in both cases (LS and PC) will not be affected since there is no added power generation.

1) Load shifting

In this case, since the load shape depends on the value of shifting factor N, ENS will also be a function of the shifting factor N. Fig 8 shows the ENS for the system versus the shifting factor. It can be seen from that figure that, unlike the commercial and the industrial loads, the residential load did not show any significant improvement. The reason lies in the fact th-

TABLE III. INTERRUPTIONS INFORMATION

Interruption No.	Date	From	To
1	6/15/2003	06:00 a.m.	10:00 a.m.
2	7/9/2003	03:00 a.m.	10:00 a.m.
3	8/25/2003	03:00 p.m.	08:00 p.m.
4	10/15/2003	10:00 a.m.	03:00 p.m.
5	10/30/2003	09:00 a.m.	12:00 p.m.
6	11/8/2003	09:00 a.m.	03:00 p.m.

TABLE IV. RELIABILITY INDICES – FIRST STAGE- BASE CASE

	Unavailability (hrs)	ENS p.u.
Residential Load	30	15.56
Commercial Load	30	18.54
Industrial Load	30	24.83

TABLE V. RELIABILITY INDICES - SECOND STAGE – WT AND PV

	ENS p.u.
Residential Load	2.58
Commercial Load	5.73
Industrial Load	8.30

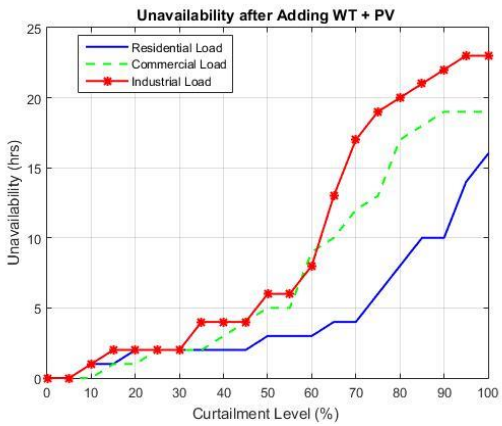

Fig 7 . Unavailability vs Curtailment Level (WT and PV)

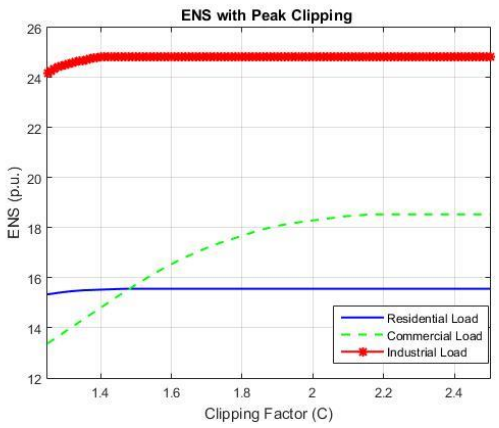

Fig 9. ENS vs. Clipping Factor

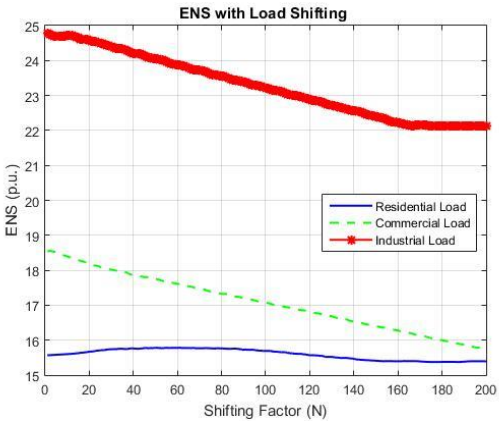

Fig 8. ENS vs. Shifting Factor

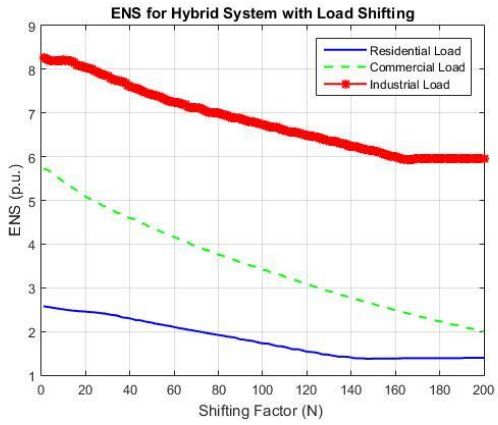

Fig 10. ENS vs. Sifting Factor - Hybrid System

-at ENS depends on load curve and failure time. If the failure time occurs at a peak, ENS will improve. Otherwise, if the fail occurs at off-peak times, ENS will increase. This is because load shifting moves amounts of load from on-peak times to off-peak times. In more practical cases, failures are more likely to happen at peak times, which means that load shifting will definitely decrease the ENS

2) Peak clipping

In this method, the ENS will depend on the clipping factor. A low clipping factor means a large amount of peak load is clipped (conserved). Hence, if the fail occurs at a peak, a low clipping factor yields low ENS and a high clipping factor results in a small or no change in the ENS. This can be seen clearly in Fig. 9, where the ENS is graphed versus the clipping factor.

D. Stage4. Integrating renewable energy and demand side management

In this stage, the impact of DSM on the reliability of the system including hybrid renewable power is studied. Both load shifting and peak clipping methods are implemented.

1) Load Shifting with hybrid renewable system

Comparing the values of ENS in Table V with the values indicated in Fig. 10, it can be seen that DSM improves the reliability of the hybrid system. As the shifting factor is increased (higher effectiveness of DSM), ENS is decreased.

Fig. 11 show the unavailability versus shifting fact-

-or at 75% level of curtailment. It can be seen that by interchanging the shifting factor, the unavailability can be affected positively or negatively. In some cases, when failures occur at off-peak periods, increasing the shifting factor will cause the unavailability to increase since more load is moved to these periods. On the other hand, if all failures occur during peak periods, increasing the shifting factor will further improve the availability for the same reason (more load is now moved from these periods). Since in our case some faults took place at peak times and others at off-peak times, altering the shifting factor may increase or decrease the hours of unavailability depending on the amount of lost load at each fault. Residential, commercial, and industrial loads have peaks at different times with different amounts, which cause the rise and fall in Fig. 11 Generally, comparing the base case (shifting factor=0) with the maximum case (shifting factor=200), the unavailability of the hybrid system decreased in all sectors.

2) Peak clipping with hybrid renewable system

The ENS for the hybrid system is shown in Fig. 12 as a function of the clipping factor. The commercial load shows the best result, which indicates that most of the faults occurred at commercial peak times.

Fig. 13 shows the unavailability versus clipping factor at 75% level of curtailment. It can be certainly realized that in contrast to the load shifting method, peak clipping can never negatively impact the figure of unavailability. It either improves it, or it does not chan-

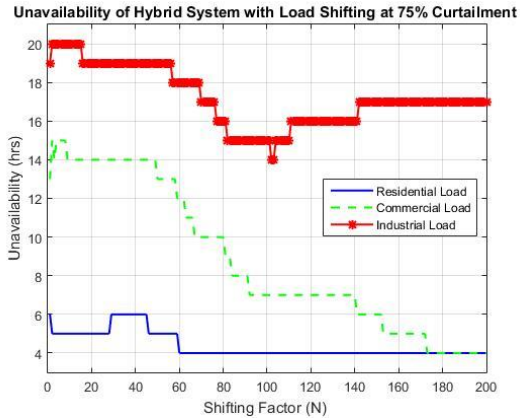

Fig 11. Unavailability vs. Shifting Factor - 75% Curtailment

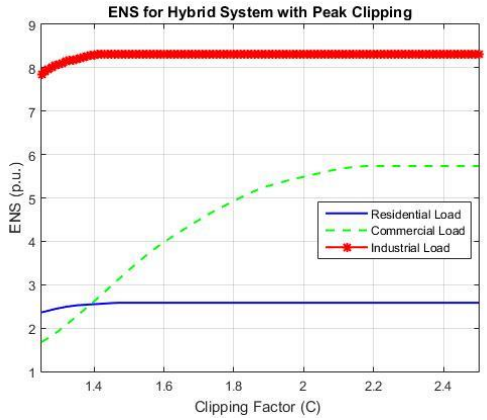

Fig 12. ENS vs Clipping Factor - Hybrid System

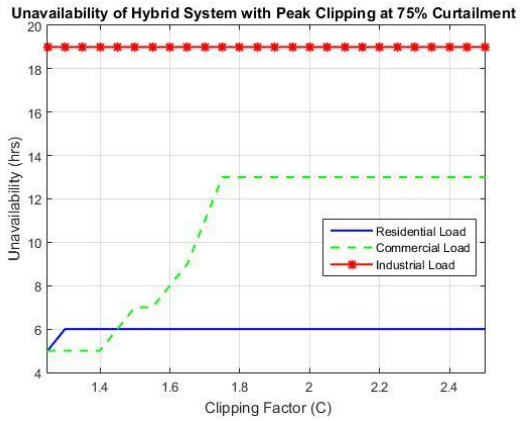

Fig 13. Unavailability vs. Clipping Factor - 75% Curtailment

-ge it as in the case of the industrial load in Fig. 13.

V. Conclusions

The reliability of a local load, including residential, commercial, and industrial sectors, was examined in four stages. These are, base stage, hybrid renewable system stage, DSM stage, and finally, combining the hybrid system with DSM. At each stage, the reliability was assessed in terms of unavailability in hours and ENS. From the study results, ENS decreased by 83%, 69%, and 66% for the residential, commercial, and industrial loads, respectively, after integrating the hybrid system. Two DSM types were introduced, load shifting and peak clipping. The ENS decreased as we apply more DSM. Finally, after combining RE with DSM in stage four, the reliability of the local load was further improved depending on DSM factors. For example, at shifting factor=200, 48%, 66%, and 27% decrease in ENS for the residential, commercial, and industrial loads were measured compared to the RE stage excluding DSM (stage 2). In general, after studying all the four stages, it was recorded that integrating RE or applying DSM highly impact the level of reliability. Moreover, combining the two aspect simultaneously, as the case in future smart grids, results in more enhancement to the level of reliability and dependency.

References

[1] Huang, Dange, Roy Billinton, and Wijarn Wangdee. "Effects of demand side management on bulk system adequacy evalua-tion." Probabilistic Methods Applied to Power Systems (PMAPS), 2010 IEEE 11th International Conference on. IEEE, 2010.

[2] Celli, G., Ghiani, E., Mocci, S., Pilo, F., Pazzola, E., "Demand Side Management as a support to distributed generation in active networks." Electricity Distribution, 2005. CIRED 2005. 18th International Conference and Exhibition on. IET, 2005.

[3] Chenye Wu, Hamed Mohsenian-Rad, Jianwei Huang and Yuex-uan Wang, "Demand Side Management for Wind Power Integra-tion in Microgrid Using Dynamic Potential Game Theory," GLOBECOM Workshops (GC Wkshps), 2011 IEEE.

[4] A. Sankarakrishnan, R. Billinton, "Sequential Monte Carlo simu-lation for composite power system reliability analysis with time varying loads," IEEE Transactions on Power Systems, v. 10, no. 3, August 1995, pp. 1540-1545.

[5] Y. Aslan, S. Yavasca and C. Yasar, "Long Term Electric Peak Load Forecasting of Kutahya using Different Approaches," In-ternational Journal on Technical and Physical Problems of Engi-neering, June 2011.

[6] Hao Jing, Liu Dawei, Li Zhenxin, Chen Zilai and Kong Lingguo, "Power System Load Forecasting Based on Fuzzy Clustering and Gray Target Theory," International Conference on Future Energy, Environment, and Materials 2012.

[7] Huang Wei, He Zijun and Fengli, "Reliability Evaluation of Microgrid with PV-WG Hybrid System," Henan electric power company, Henan, China 2011.

[8] AlOwaifeer, M., AlMuhaini, M., & AlSaggaf, A. (2015, June). The impact of load management and renewable DG on the service restoration of future power distribution systems. In Environment and Electrical Engineering (EEEIC), 2015 IEEE 15th International Conference on (pp. 1789-1794). IEEE.

[9] Allan, R. N., Billinton, R., Sjarief, I., Goel, L., & So, K. S. (1991). A reliability test system for educational purposes-basic distribution system data and results. Power Systems, IEEE Transactions on, 6(2), 813-820.